Microbial Pathogenesis 81 (2015) 6–15

Contents lists available at ScienceDirect

Microbial Pathogenesis

journal homepage: www.elsevier.com/locate/micpath

Deciphering the protein interaction in adhesion of *Francisella tularensis* subsp. *holarctica* to the endothelial cells

Elena Bencurova [a], Andrej Kovac [b], Lucia Pulzova [a], Miklós Gyuranecz [c], Patrik Mlynarcik [a], Rastislav Mucha [b], Dimitrios Vlachakis [d], Sophia Kossida [d], Zuzana Flachbartova [a], Mangesh Bhide [a, b, *]

[a] Laboratory of Biomedical Microbiology and Immunology, Department of Microbiology and Immunology, University of Veterinary Medicine and Pharmacy in Kosice, 041 81 Kosice, Slovakia
[b] Institute of Neuroimmunology, Slovak Academy of Sciences, 845 10 Bratislava, Slovakia
[c] Institute for Veterinary Medical Research, Centre for Agricultural Research, Hungarian Academy of Sciences, H-1581 Budapest, Hungary
[d] Bioinformatics & Medical Informatics Team, Biomedical Research Foundation, Academy of Athens, Athens 11527, Greece

ARTICLE INFO

Article history:
Received 20 August 2014
Received in revised form
26 February 2015
Accepted 9 March 2015
Available online 11 March 2015

Keywords:
Endothelial cells
Francisella
ICAM-1
Type IV pili

ABSTRACT

Extracellular form of *Francisella* is able to cross various cell barriers and invade multiple organs, such as skin, liver, lung and central nervous system. Transient adhesion of *Francisella* to endothelial cells may trigger the process of translocation. In this report, we showed that *Francisella tularensis* subsp. *holarctica* (*Fth*) is able to adhere to the endothelial cells, while ICAM-1 may serve as an adhesion molecule for *Fth*. Pull down and affinity ligand binding assays indicated that the PilE4 could be the probable ligand for ICAM-1. Further deciphering of this ligand:receptor interaction revealed that PilE4 interacts with Ig-like C2-type 1 domain of ICAM-1. To corroborate the role of PilE4 and ICAM-1 interaction in adhesion of extracellular form of *Fth* to endothelial cells, ICAM-1 was blocked with monoclonal anti-ICAM-1 antibody prior to the incubation with *Fth* and numbers of adherent bacteria were counted. Blocking of the ICAM-1 significantly reduced (500–fold, $P < 0.05$) number of adherent *Fth* compared to unblocked cells. PilE4:ICAM-1 interaction unfolded here may provide a new perspective on molecules involved in the adhesion of extracellular form of *Francisella* to endothelial cells and probably its translocation across endothelial barriers.

1. Introduction

Francisella tularensis, a causative agent of tularemia, is highly infectious Gram-negative facultative intracellular coccobacillus. It has been detected in more than 250 host species, including human. *F. tularensis* subsp. *tularensis* can cause severe infection and can be fatal if left untreated. It is to be noted that *Francisella* can readily disseminate into various organs and sporadically invade the CNS. The presence of *F. tularensis* subsp. *holarctica* (*Fth*) in the brain tissues has been reported previously [1–3]. Pathogens exploit several strategies to cross the endothelial barrier in the microvalsculature and disseminate into various organs. They use three major routes to cross the endothelial barrier: 1. transcellular, 2. paracellular, and 3. so-called Trojan horse mechanism (by means of infected phagocytes) [4,5]. Extracellular pathogens translocate the barrier via transcellular or paracellular routes that involve series of events like transient tethering-type associations of pathogen to endothelial cells, short-term dragging interactions and a stationary adhesion. These interactions evoke signalling events in endothelial cells, which may lead to the remodulation of cytoskeleton and may facilitate a passage for extracellular microorganisms to cross the barrier [5,6].

Francisella prefers intracellular environment, however its significant extracellular phase has been documented in experimentally infected mice [7]. In majority of the infected mice, *Francisella* recovered from the blood was in plasma rather than leukocytes. Authors found this distribution irrespective of size and route of inoculum, time after inoculation or virulence of the infecting strain [7]. It was also demonstrated that extracellular *Francisella* readily

* Corresponding author. Laboratory of Biomedical Microbiology and Immunology, Department of Microbiology and Immunology, University of Veterinary Medicine and Pharmacy in Kosice, Komenskeho 73, 041 81 Kosice, Slovakia.
E-mail address: bhidemangesh@gmail.com (M. Bhide).

http://dx.doi.org/10.1016/j.micpath.2015.03.007
0882-4010/

adheres to the endothelial and epithelial cells [8–10]. Hitherto, molecular mechanisms underlying adhesion of *Francisella* to the endothelial cells and its translocation across the endothelial barrier are not fully studied.

Bacterial adhesion to the endothelial cells is usually regarded as a two-step process: 1) initial adhesion (pilus mediated) and 2) intimate adhesion (involves other bacterial and cellular structures) [11]. Many pathogens have evolved diverse surface structures to interact with host cells. Among them, filamentous pili-like structures have been documented previously on the surface of *Vibrio cholerae, Pseudomonas aeruginosa, Helicobacter pylori, E. coli*, and *F. tularensis* [12,13]. Although, the function of type IV pili subunits of *F. tularensis* are still unclear, there is evidence that expression of PilT and PilF is necessary for higher virulence of LVS [14].

In the present study, we assessed ability of *F. tularensis* subsp. *holarctica* (*Fth*) to cross the endothelial barrier *in vivo* and *in vitro*. Then we set out to assess an ability of *Fth* to adhere to the endothelial cells. We also aimed to identify the receptor and ligand involved in the adhesion. Overall experiments revealed that 1. *Fth* can cross the endothelial barrier *in vivo*; 2. It can also cross the endothelial barrier *in vitro* in the absence of leukocytes; 3. It readily adheres to the endothelial cell surface; 4. It uses PilE4 (type IV pili subunit) to interact with ICAM-1 molecule and adhere on the endothelial surface.

2. Material and methods

2.1. Ethics statement

The Institute for Veterinary Medical Research, Centre for Agricultural Research, Hungarian Academy of Sciences (HAS), H-1581 Budapest, Hungary, is certified by the national accreditation of laboratory animal care. Experiment on animals was performed according to the guidelines approved by the ethical committee.

2.2. Cultivation of Francisella

F. tularensis subsp. *holarctica* (*Fth*, neuroinvasive strain isolated from the brain of European brown hare, *Lepus europaeus*; GenBank accession number GU566694.1) was cultured on enriched chocolate agar containing 1% glucose and 0.1% L-cystein at 37 °C for 4–5 days. Single colony from agar was inoculated into 100 ml of BHI medium (HI media, India) enriched with 1% glucose and 0.1% L-cystein and incubated at 37 °C for 48 h with constant shaking at 200 rpm. To inactivate bacteria, 5 ml of culture was incubated with 500 μl of gentamicin (100 μg/ml) for 24 h at 37 °C.

2.3. Bacterial cell counting

Standard CFU count was used to determine the number of bacterial cells used in various experiments. Alternatively, in some experiments bacteria-counting kit for flow-cytometry (Molecular probes, USA) or qPCR was used. Bacterial cell count obtained by flow-cytometry was correlated with CFUs. To plot a standard curve of DNA copy number of *Fth*, culture with known bacterial count (measured by flow-cytometry) was serially diluted from 5.5×10^6 to 5.5×10^1 cells/ml. DNA from 1 ml of diluted cultures was isolated with DNAzol direct kit (Molecular Research centre, USA) and qPCR was performed using qPCR Green Master mix (Jena Bioscience, Germany) and lpnA primers in iCycler IQ5 thermal cycler (Bio-Rad, USA). The cycling conditions were as follows: 94C-3 min, 40 × (94 °C-15 s, 60 °C-30 s, 72 °C-45 s) and 72 °C-7 min. Standard curve was plotted using six replicates.

2.4. Cultivation of endothelial cells and preparation of in vitro model of endothelial barrier

Primary rat brain microvascular endothelial cells were prepared from 2-week-old Wistar rats, as described previously [15]. Endothelial cell clusters were plated on fibronectin and collagen type IV coated culture dishes (for endothelial monolayer) or cell culture inserts (for *in vitro* endothelial barrier; Transwell; 1 cm^2; pore size 1 μm; BD Bioscience, USA) and cultivated as we described before [15]. In case of culture dishes, formation of confluent monolayer was assessed by microscopy. Trans-endothelial electrical resistance (TEER, ENDOHM-12 chamber, WPI Europe) was measured to assess the integrity of monolayers in *in vitro* model of endothelial barrier (in Transwells).

2.5. Adhesion of Francisella to endothelial cells: adhesion assay

One ml of *Fth* culture containing 3.6×10^6 cells was centrifuged and the pellet was washed with DMEM-F12-G medium. *Fth* cells were added to endothelial monolayer (multiplicity of infection 1) grown in culture dishes and incubated at 37 °C for 4 h. The incubation time in adhesion assay was set according to previous works [16,17]. Non-adherent *Fth* were washed with PBS and number of adherent *Fth* were measured by qPCR and CFU count. In case of qPCR, a standard curve of DNA copy number of *Fth* spiked in endothelial cell culture was plotted. In short, *Fth* cells were serially diluted from 5.5×10^6/ml to 5.5×10^1/ml. One ml of diluted culture was pelleted and spiked in the monolayer of endothelial cells. DNA from spiked cells was isolated with DNAzol and qPCR was performed as described above targeting *lpnA* gene. Standard curve was plotted using six replicates. qPCR was also performed on DNA isolated from endothelial cells without spiking. As a negative control bacteria were incubated in the wells without monolayer. Adhesion assay was performed in triplicates.

DNA from culture dishes of adhesion assay was isolated with DNAzol. Number of adherent *Fth* was calculated by using a standard curve of DNA copy numbers. Some culture dishes from adhesion assay were used for visualization of adherent *Fth*. In short, cultures were fixed with 4% paraformaldehyde, permeabilized with 0.3% Triton X/PBS for 20 min and washed with PBS. Cells were incubated in 2% solution of skimmed milk powder for 20 min. Endothelial cells stained with polyclonal rabbit anti-ZO-1 antibody (Invitrogen, Carlsbad, CA, USA) followed by secondary antibody Alexa Fluor 488 goat anti-rabbit (Invitrogen). Adherent *Fth* on endothelial cells were detected by monoclonal anti-*Francisella* antibody in mouse (Abcam, UK) and secondary antibody Alexa Fluor 546 goat anti-mouse (Invitrogen). All antibodies were diluted 1:1000.

2.6. Crossing of the endothelial barrier in vitro: translocation assay

One millilitre of the *Fth* culture containing 1×10^5 cells was centrifuged, pellet was resuspended in DMEM/F12-G medium and added to the luminal chamber of cell culture inserts containing confluent monolayer. *Francisella* cells were also added to the luminal chamber of empty cell culture inserts to assess free passage of *Fth* across the membrane. As a negative control, inactivated *Fth* were added to the luminal chamber. Inserts were incubated at 37 °C for 8 h and the contents of luminal and abluminal chambers were collected and centrifuged. Supernatant was discarded and DNA from the pellet was isolated with DNAzol and purified by phenol-chloroform-ethanol precipitation. DNA concentration was set to 20 ng/μl and used as a template for qPCR and PCR targeting *lpnA* gene as described above. An aliquote of luminal and abluminal contents was also subjected to CFU count. The endothelial monolayer was checked microscopically before and after the experiment to verify integrity of the cell layer. TEER was also measured to

Table 1
Primers used in the study.

Primer	Primer sequence 5′-3′	Accession no.
A) Identification of *Francisella*		
lpnA F:	GGAGCYTGCCATTGTAATCTTAC	M32059.1
lpnA R:	GYAGGTTTAGCKAGCTGTTCTA	M32059.1
B) Construction of recombinant form of proteins in yeast and *E. coli* expression systems		
ICAM-1F (yeast):	AAAAAGCTTGGTGCTCAGGTATCCATC	NM_012967
ICAM-1R (yeast):	GTTTCTAGAGGGGAGGCGGGGCTTGTAC	NM_012967
PilE1F:	AAAGGATCCGCGATCCCGATGTACTCTAAC	AAX14621.1
PilE1R:	ATAGTCGACTCTCCCTTCTATTACTTGAGAT GCTGATACACCTGA	AAX14621.1
PilE3F:	AAAGGATCCATCCCAGCGTATTCAAACTAT	AAX14621.1
PilE3R:	TAAGTCGACTCTCCCTTCTATAGCGTCTTGTT CAACTAT	AAX14621.1
PilE4F:	AAAGGATCCAAAGGAATGACAATCTCAGAG	AY788838.1
PilE4R:	ATAGTCGACTCTCCCTTCTATCCCAATCATT ATGAGCAT	AY788838.1
PilE5F:	AAAGGATCCGCTATTCTTGCATCTATAGGT	AY788839
PilE5R:	ATAGTCGACTCTCCCTTCTATATTCCAGCAT TCAGCAGG	AY788839
PilWF:	CGAGGATCCACTCCAGAAACCCCTACTCGT	AM233362
PilWR:	ATAGTCGACTCTCCCTTCTATATCCTCTTGAT CGGCTGC	AM233362
C) OE-PCR		
rICAM-1-5 F:	**overlap**GGTGCTCAGGTATCCATC	NM_012967
rICAM-1-5 R:	**overlap**AGGGGGGAGGCGGGGCTTGTAC	NM_012967
Ig-like C2-type 1 F:	**overlap**AGGTGCTCAGGTATCCATCCAT	NM_012967
Ig-like C2-type 1 R:	**overlap**AGGTCCACTCGCTCTGGGAA	NM_012967
Ig-like C2-type 2 F:	**overlap**ACAGCAGGTGGGCAAGAAC	NM_012967
Ig-like C2-type 2 R:	**overlap**AGGAGGTCAGGGGTGTC	NM_012967
Ig-like C2-type 3 F:	**overlap**ACCACAAGGGCTGTCACTGTTC	NM_012967
Ig-like C2-type 3 R:	**overlap**AGGGTCTTCTCCATCTCCAGGGTCTG	NM_012967
Ig-like C2-type 4 F:	**overlap**AATCCTGACCCTGAGCCAG	NM_012967
Ig-like C2-type 4 R:	**overlap**AGGGACTTCCCATCCACCTCCAA	NM_012967
Ig-like C2-type 5 F:	**overlap**TGGACAAGAAGGACTGC	NM_012967
Ig-like C2-type 5 R:	**overlap**AGGTCCCTGGTGATACTCCC	NM_012967

Restriction enzyme site is indicated as underlined. Overlaps are the nucleotide sequences used in the OE-PCR; details of this sequences are described in our open access publication [23].

before and after incubation with *Fth*. The experiment was made in triplicates.

2.7. Assessment of crossing of the blood–brain barrier in vivo: CNS invasion

Six Wistar rats (Charles River Laboratories Inc., USA, ~300 g) were infected via intra peritoneal route with 5×10^5 *Fth*. One Wistar rat was used as a negative control and was injected with normal saline. Moribund rats were euthanized with CO_2. Three weeks after challenge non-infected rat was sacrificed. After gross pathological examination, tissue samples (cerebrum and cerebellum) were collected and fixed in 8% neutral buffered formalin. Four-micron thick sections of formalin-fixed and paraffin-embedded tissue samples were stained with hematoxylin and eosin, and examined by light microscopy. For immunohistochemistry, sections were dewaxed and incubated in 3% H_2O_2 solution for 10 min and in 2% solution of skimmed milk powder for 20 min. The sections were incubated overnight at 4 °C with anti-*Fth* hyperimmune serum (Lab-Nyúlkft., Hungary) diluted 1:20,000 in PBS. Antibody binding was detected with anti-rabbit antibodies with HRP-labelled polymer as per manufacturer's instructions (EnVisionTM + Kit; Dako, Denmark). Non-infected rat brain served as negative control. For some sections antiserum was replaced by PBS to rule out the possibility of any nonspecific binding.

2.8. Identification of the probable receptor on endothelial cells interacting with ligand of Francisella: ligand capture assay

Membrane proteins of endothelial cells and proteins of *Fth* were isolated with ProteoJet membrane protein extraction kit (Thermo Scientific, USA) as per manufacturer's instructions. Proteins of *Fth* were immobilized on nitrocellulose membrane; non-specific binding sites were blocked with blocking agent (Pierce) and hybridized with membrane proteins of the endothelial cells. After stringent washing, interacting proteins were eluted and resolved on SDS-PAGE. A methodology including relevant negative controls is detailed in our previous work [15]. Protein band from SDS-PAGE was identified by peptide mass fingerprinting (PMF) as described previously [18].

2.9. Overexpression of rICAM-1

Protein coding region of rat ICAM-1 (26th to 545th amino acids), was amplified (accession number: NM_012967; primers in Table 1), PCR product was digested with *XbaI* and *HindIII* enzymes (Thermo Scientific, USA) and cloned into the pYEBME-1 expression vector (patent pending – No. 000892011, Slovak patent office). Detailed description of the vector, all steps in cloning, transformation and overexpression of the proteins are described in our previous work [19]. Overexpressed 6x His-tagged ICAM-1 was purified using Ni-NTA (Qiagen, Netherlands) under native conditions as per the manufacturer's instructions.

2.10. Identification of interacting partner of rICAM-1 by pull-down assay on magnetic beads

Purified rICAM-1 was incubated for 1 h with magnetic beads loaded with Co^{2+} metal ions (MB-IMAC kit, Bruker-Daltonics, Germany). After incubation, beads were placed in a magnetic separator

and washed with washing buffer provided in the kit. Beads were hybridized with membrane proteins of *Fth* resuspended in binding buffer provided in the kit or only in binding buffer as negative control. After overnight incubation at 4 °C, tube was placed into the magnetic separator and supernatant was discarded. Beads were washed with wash buffer and the tube was placed again in the magnetic separator to collect beads on one side. Proteins bound to rICAM-1 were eluted with elution buffer provided in the kit, fractionated on SDS-PAGE, visualized by coomassie blue and identified by PMF [18].

2.11. Preparation of recombinant forms of proteins of Francisella

Protein coding regions of PilE1, PilE3, PilE4, PilE5 and PilW were amplified by PCR and amplicons were gel purified. Primers are shown in Table 1. Amplicons were digested with *BamHI* and *SalI* enzymes (Thermo Scientific, USA) and ligated into previously digested vector pQE-30UA-GFP (in house modified pQE-30 vector from Qiagen, GFP tag inserted at C terminus of protein of interest). Purification, transformation, overexpression of proteins and lysis of bacteria was performed as described previously [20]. Lysate containing His-tagged pili subunits were purified with metal affinity chromatography (Clontech, USA).

2.12. Affinity ligand binding assay to assess binding ability of pili subunits to endothelial proteins

Membrane proteins of endothelial cells were extracted by ProteoJet Membrane Protein Extraction kit and fractionated on NuPAGE 2D well polyacrylamide gel (Invitrogen, 400 μg of proteins per well). Proteins were electrotransferred onto a nitrocellulose membrane and membranes were cut into vertical strips. Strips were blocked in 2% BSA-TTBS and incubated with rPilE1, rPilE3, rPilE4, rPilE5 and rPilW resuspended in 0.5% BSA-TTBS. Bound rPil subunits were detected by Ni-HRP conjugate diluted at 1:5000 in 1% BSA-TTBS for 1hr and visualized with Super-Signal West Pico chemiluminiscence substrate (both Pierce, Thermo Scientific, USA). Signals were captured on X-ray film.

2.13. Line blotting for assessment of interaction between Francisella ligands and ICAM-1

rICAM-1 diluted in TBS was loaded on a PVDF membrane (Immobilon P, Millipore, USA) placed into the Miniblotter® using simple diffusion method [21]. Concentration of rICAM on the membrane was 100 ng/mm^2. Membrane was dismantled from Miniblotter, blocked in 1% BSA-TTBS and then mounted again into the Miniblotter, however with the lanes carrying protein rotated at 90°. Lanes were then filled with each of the GFP-tagged rPil subunits diluted in TBS to a final concentration 0.5 mg/ml. As negative control, one lane was filled only with TBS. Miniblotter was incubated for 1 h, lanes were washed with TTBS and anti-GFP HRP antibody (Pierce, Thermo Scientific, USA, 1:10,000 in 1.5% BSA-TTBS) was loaded in each lane. After 1 h of incubation membrane was taken out of Miniblotter and subjected for chemiluminiscence reaction as described above.

2.14. Pull-down assay on affinity beads

Recombinant PilE4 was bound on metal affinity beads according to the manufacturer's instructions (Clontech, USA). After binding, beads were washed with wash buffer [15] and incubated overnight at 4 °C with membrane proteins of endothelial cells. Beads were washed twice with wash buffer and twice with MilliQ water. Protein complex was eluted and proteins were identified by PMF as described in our publications [18,22]. As a negative control, membrane proteins of endothelial cells were incubated directly with metal affinity beads. As an input control, rPilE4 was bound on affinity beads, washed, eluted and subjected to MALDI mass spectrometry.

2.15. Assessment of interaction between PilE4 and ICAM-1 domains

Six truncated forms of ICAM-1 (full-length ICAM-1 and each of five Ig-like C2-type domains) were constructed by overlap-extension (OE) PCR and *in vitro* translation exactly as described before by us [23]. Primers used in OE PCR are depicted in Table 1. Truncated ICAM-1 fragments were immobilized on PVDF membrane. Membrane was blocked in 2% BSA-TTBS for 1 h and then incubated with rPilE4 (70 ng of total protein, resuspended in 1% BSA-TTBS) for 1 h. After incubation membrane was washed and incubated with Ni-HRP and subjected for chemiluminiscence as described above. As an input control, ICAM-1 fragments were immobilized on a membrane and detected with anti-Myc HRP antibody (diluted at 1:10,000 in 1% BSA in TTBS) and chemiluminiscence substrate. As a negative control, membrane with ICAM-1 fragments was incubated with Ni-HRP conjugate for 1 h and subsequently subjected to chemiluminiscence.

2.16. Blocking of ICAM-1 and its influence on Fth adhesion

Endothelial cells were cultivated in 6 well plates and pre-incubated with anti-ICAM-1 antibody in mouse (0.25 μg/cm^2, Abcam) for 45 min before addition of *Fth* (MOI − 1; 3.6 × 10^6 cells per well) suspended in DMEM-F12 medium. *Francisella* were incubated for 4 h at 37 °C. Non-adherent *Fth* were washed with PBS and genomic DNA was isolated by DNAzol. qPCR based on amplification of *lpnA* gene was performed as described above. The endothelial cells without pre-incubation were served as positive control. Endothelial cells incubated only with anti-ICAM-1 antibody were used as negative control. Wells without endothelial cell monolayer incubated with ICAM-1 and then *Fth* were also served as negative control. Experiment was conducted in triplicates. Paired t-test (STATGRAPHICS plus 5.1) was used to assess variation in the adhesion of *Fth* on the blocked and unblocked endothelial cells. Simultaneously, adherent *Fth* were also calculated with CFU count. In some wells, pre-incubation of endothelial cells with non-relevant antibodies (anti-CD40 antibody and anti-ZO-1 antibody, both in the mouse, same subclass, Abcam) was also performed to rule out non-specific blocking that may occur due to IgG molecule.

2.17. Homology modelling and docking

The homology modelling for PilE4 was performed using Modeller [24]. The crystal structure of the glycolate oxidase (PDB entry: 1AL7), MutS alpha (PDB entry: 208B) and renalase (PDB entry: 3QJ4) were used for the modelling of PilE4. As a template for the modelling of the Ig-like C2-type 1 domain the crystal structure of the human intercellular adhesion molecule-1 (PDB entry: 1IAM) was used. Energy minimization and molecular dynamics simulations were performed as described previously [25]. 3D structural conformation of ICAM-1 and PilE4 was performed using the docking suite ZDOCK, version 3.0 [26].

3. Results

3.1. Adhesion of Fth to endothelial cells and it crossing across the endothelial barrier

Adhesion of bacteria to endothelial cells is a crucial step in its

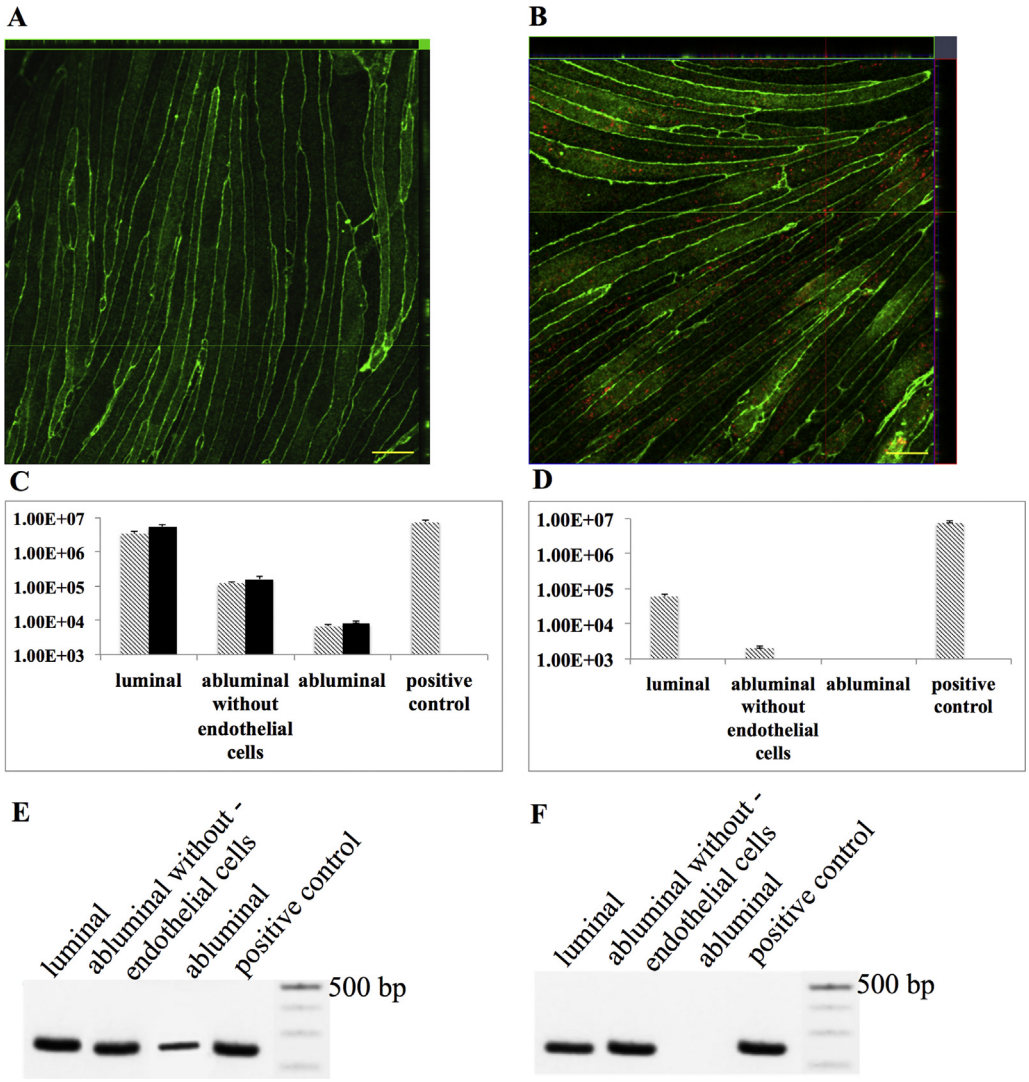

Fig. 1. Adhesion of *Francisella* on endothelial cells and translocation across endothelial barrier. Panels A represents confluent monolayer of endothelial cells stained with polyclonal rabbit anti-ZO-1 followed by secondary antibody Alexa Fluor 488 goat anti-rabbit. Panel B depicts adherent *Fth* (red dots) on endothelial cells (magnification 100x) detected by monoclonal anti-*Francisella* antibody and Alexa Fluor 546 goat anti-mouse secondary antibody. Please note that majority of the bacteria were seen extracellularly, however some of them were also intracellular. In both panel A and B Scale bar = 50 μm. Panel C and E represents translocation assay performed with live bacteria. Panel D and F represents translocation assay performed with inactivated bacteria. *Francisella* was added to the luminal chamber of endothelial barrier and the presence of *Francisella* in the luminal and abluminal chamber was detected by qPCR (grey columns) or CFU (dark columns). Positive control – genomic DNA of *Francisella* used in qPCR. (For interpretation of the references to colour in this figure legend, the reader is referred to the web version of this article.)

paracellular or transcellular translocation across the barrier. In adhesion assay performed with qPCR, we found an average of 4.7×10^5 (standard deviation 1.1×10^3) adherent *Fth* on endothelial cells, while 3.9×10^5 (standard deviation 2.1×10^3) CFU were observed on enriched chocolate agar. *Francisella* adhered on the endothelial cells are shown in panel B of Fig. 1. When *Francisella* were incubated in the culture dishes without endothelial cell monolayer, negligible number of *Francisella* (1.2×10^2 standard deviation 24.6, qPCR or 0.6×10^2 standard deviation 14, CFU), were detected.

Pathogens use various routes of translocation to cross endothelial barriers like transcellular, paracellular and/or by means of infected phagocytes. Molecular mechanisms underlying the passage of *Francisella* across the endothelial barrier are not yet clear. To reveal an ability of extracellular form of *Francisella* to cross the endothelial barrier, an *in vitro* model of endothelial barrier was constructed and a translocation assay was performed. Pathogens that solely rely on Trojan horse mechanism (like strictly intracellular pathogens) fail to translocate *in vitro* model of the endothelial barrier in the absence of leukocytes.

Prior to preparation of endothelial barrier on cells culture inserts (Transwell), free movement of live *Fth* across the cell supporting membrane was necessary to assess. This was achieved by incubating live and inactivated *Fth* on cell culture inserts without endothelial cells. The presence of live *Fth* in abluminal chamber (Fig. 1, panels C to F) confirmed that supporting membrane poses no hindrance for bacterial movement from luminal to abluminal chamber.

In the translocation assay performed *in vitro*, we found presence of live *Fth* in abluminal chambers (Fig. 1, panels C and E), however, *Fth* inactivated with gentamicin were unable to cross the barrier and get entry into the abluminal chambers (Fig. 1, panels D and F). This indicates that *Fth* may possess an ability to cross the endothelial barrier without help of leukocyte, either via transcellular or paracellular route of translocation. No rupture of the endothelial cells layer was noticed under the microscope after translocation

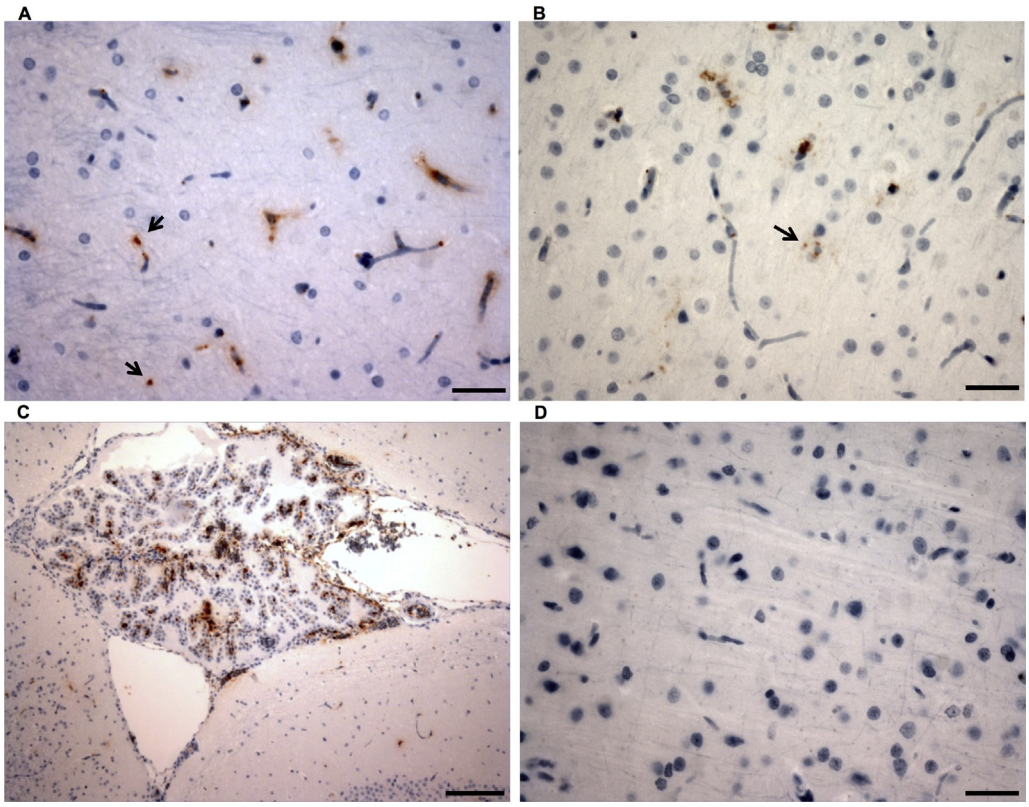

Fig. 2. Immunostaining of *Fth* in the brains of infected rats. Positive immunostaining with anti-*Francisella* antibody (arrows) was observed in the parenchyma of frontal cortex (A and B). Extensive positive immunohistochemical staining was observed in the choroid plexus (C). No staining was observed in the brains of non-infected animals (D). Scale bar = 20 μm (A, B, D), 200 μm (C).

assay. The TEER value remained unchanged before and after translocation assay (before incubation with *Fth* – TEER 11 ± 0.21 Ωcm^2, after incubation - TEER 12 ± 0.45 Ωcm^2).

Blood-brain barrier, lined by brain microvascular endothelial cells, is considered as the most difficult obstacle for the pathogens. Thus we tested an ability of *Fth* to cross the endothelial barrier in rat and invade the CNS. Multiple *Fth* cells were detected within the lumen of the blood vessels as well as in the extravascular tissues mainly in the parenchyma of the frontal cortex (Fig. 2, panels A and B). Immunohistochemistry also revealed presence of bacteria in the choroid plexus of the infected animals (Fig. 2, panel C).

Overall results indicated that *Fth* could cross the endothelial barrier, eventually also the blood–brain barrier. Results also showed the ability of *Fth* to cross the endothelial barrier *in vitro* in the absence of leukocytes, which indicates that *Fth* might not entirely rely only on Trojan horse mechanism, but might also exploit paracellular or transcellular way.

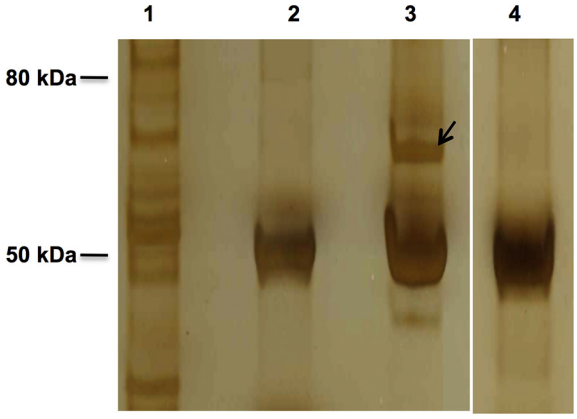

Fig. 3. Ligand Capture Assay. Proteins of *Fth* fractionated by PAGE and electro-transferred on the nitrocellulose membrane were hybridized with the surface proteins of endothelial cells. After hybridization, interacting proteins were stripped and concentrated. Proteins were subsequently fractionated on SDS-PAGE and visualized by silver staining. Lane 1, *Fth* membrane proteins; lane 2, negative control # 1 – nitro-cellulose membrane carrying proteins of *Fth* was blocked and subjected for stripping, band at 50 kDa indicates protein present in blocking buffer; lane 3, proteins of the endothelial cells hybridized with proteins of *Fth* on membrane, interacting proteins were stripped, arrow depicts the band that was cut out and analyzed with mass spectrometry; lane 4 - negative # 2 - nitrocellulose membrane without proteins of *Fth* was blocked and incubated with the proteins of endothelial cells. A single band at 50 kD indicates that there is no non-specific interaction between the blocking agent and the proteins of endothelial cells.

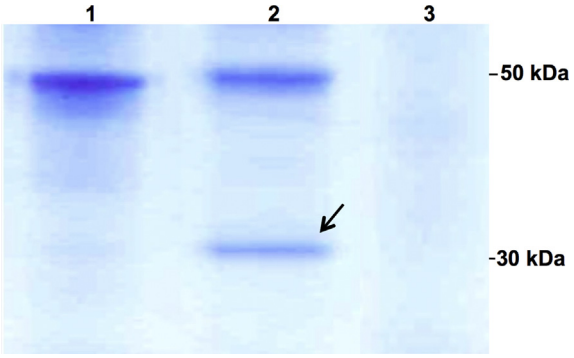

Fig. 4. Identification of *Fth* protein interacting with ICAM-1. Lane 1, rICAM-1 was captured on MB-IMAC beads and eluted; lane 2, rICAM-1 was captured on MB-IMAC beads, hybridized with membrane proteins of *Fth* and complex was eluted; lane 3, rICAM-1 was excluded from assay. Arrow indicates the protein band was cut from the gel and subjected for peptide mass fingerprinting.

3.2. ICAM-1: putative adhesion molecule for Fth on endothelial cells

Adhesion of bacteria on the endothelial cell surface is a crucial step to initiate the process of paracellular or transcellular translocation. A ligand capture assay was performed to identify a receptor on the endothelial cells involved in the adhesion of *Fth*. After hybridization of membrane proteins of endothelial cells with the proteins of *Fth*, interacting protein candidates were stripped and separated on PAGE, in which a prominent band at approximately 60 kDa was observed (Fig. 3, lane 3). In case of negative controls (Fig. 3, lanes 2 and 4), a single band of the blocking agent (single protein blocking agent) indicated that none of the proteins from the endothelial cells interacted nonspecifically to the blocking agent. PMF performed for the excised protein band (60 kDa) revealed that ICAM-1 (gi:6981068, 5 peptides matched, 94 score, significance threshold <0.05) might be the probable receptor for *Fth* on the endothelial cells.

3.3. Type IV pili subunit of Fth interacts with rICAM-1

To identify the ligand of *Fth* interacting with ICAM-1, recombinant ICAM-1 was overexpressed, immobilized on magnetic metal affinity beads and hybridized with membrane proteins of *Fth*. Interacting proteins were eluted and separated on polyacrylamide gel. A prominent band at 35 kDa (Fig. 4, lane 2) was excised and subjected for protein identification. Interestingly, peptide mass fingerprinting and BLAST search for this protein revealed multiple protein candidates with high probabilities: 1. type IV pili fiber building block protein (type IV pilus assembly protein PilE4, gi:89255780, 7 mass values matched, 75 score), 2. Type IV fimbrial protein PilW (gi:336446354, 6 mass values matched, 74 score).

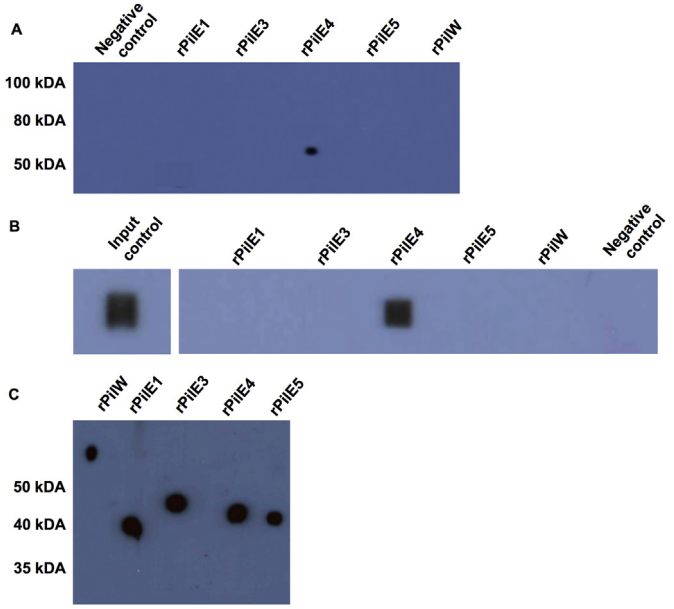

Fig. 5. Interaction between endothelial cells receptor (ICAM-1) and type IV pili subunits. Panel A – Endothelial cells proteins were separated by SDS-PAGE, transferred on nitrocellulose membrane and hybridized with recombinant PilE1, PilE3, PilE4, PilE5 and PilW subunits. Negative control, recombinant proteins were omitted from overall protocol. Panel B – rICAM-1 was immobilized on Immobilon membrane and hybridized with recombinant PilE1, PilE3, PilE4, PilE5 and PilW. Interaction was detected with anti-GFP antibody. As an input control, rICAM-1 was detected with Ni-HRP conjugate. Negative control, rICAM-1 incubated with anti-GFP antibody to rule out any non-specific antibody binding. Panel C – input control for recombinant type IV pili subunits. Proteins were separated on SDS-PAGE, electrotransferred and detected with Ni-HRP conjugate.

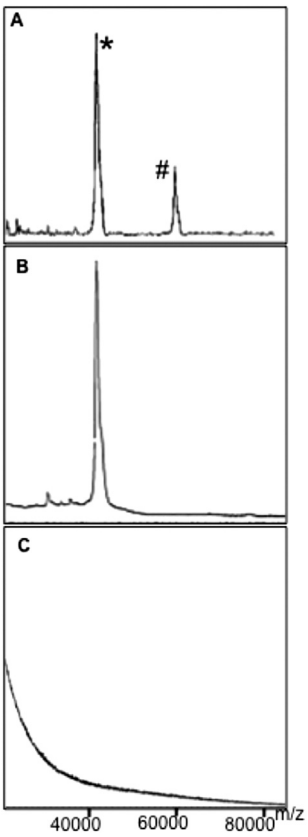

Fig. 6. Interaction between rPilE4 and proteins of endothelial cells. Panel A – rPilE4 was bound on the metal affinity beads and incubated with membrane proteins of endothelial cells; * peak shows rPilE4, # peak corresponds to the mass of ICAM-1. Panel B – input control, rPilE4 bound on the metal affinity beads was eluted and subjected on MALDI-TOF analysis. Panel C – negative control, proteins of endothelial cells were hybridized with metal affinity beads, eluted and subjected for mass spectrometry. Proteins from both peaks (* and #) in panel A were identified by peptide mass fingerprinting as PilE4 and ICAM-1.

Many bacteria use type IV pili to adhere to the host cells, however its role in the adhesion of *Francisella* to the host cells is still unclear. The role of the PilW, a second protein candidate identified in peptide mass fingerprinting and BLAST search, is neither fully understood. Owing to the fact that function of IV pili subunits is still matter of debate, we assessed if other pili subunits (PilE1, PilE3 and PilE5) may interact with ICAM-1. Series of experiments was performed to assess their ability to adhere to endothelial receptor. In the affinity ligand binding assay, ICAM-1 was fractionated from endothelial cell proteins on polyacrylamide gel, transferred on the nitrocellulose membrane and hybridized with recombinant pili subunits (PilE1, PilE3, PilE4, PilE5 and PilW). We found that among various pili subunits only rPilE4 possess affinity to ~60 kDa protein of endothelial cells (Fig. 5, panel A). To validate this interaction, a line blotting was performed, in which both ligand and receptors were in recombinant form. rICAM-1 was immobilized on a membrane and hybridized with recombinant pili subunits. This experiment confirmed that only PilE4 binds ICAM-1 (Fig. 5, panel B). Affinity of PilE4 to ICAM-1 was also proved by pull-down assay, wherein we noticed the presence of two peaks: first at 41.9 kDa corresponding to the molecular mass of rPilE4 and the second at the corresponding mass of ICAM-1 (Fig. 6, panel A). No peak was noted when proteins of endothelial cells were incubated with affinity beads without prior PilE4 loading (Fig. 6, panel C), which indicates that none of these proteins possesses non-specific affinity to beads.

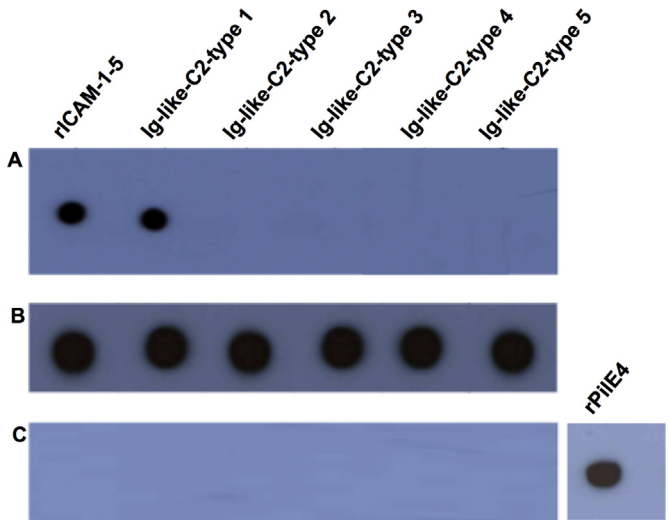

Fig. 7. Interaction between rPilE4 and domains of ICAM-1. Panel A – rICAM-1 and its domains were immobilized on PVDF membrane, hybridized with purified rPilE4 and detected with Ni-HRP conjugate. Panel B – rICAM-1 domains were immobilized on PVDF membrane and hybridized with anti-Myc-HRP antibody (input control). Panel C – rICAM-1 domains and rPilE4 were immobilized on PVDF membrane and hybridized with Ni-HRP conjugate.

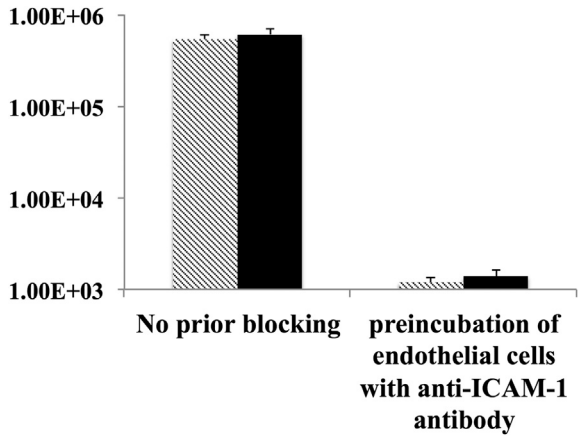

Fig. 8. Inhibition of adhesion of *Francisella* to endothelial cells. Numbers of adherent *Francisella* to endothelial cells without and with preincubation of endothelial cells with anti-ICAM-1 antibody. Numbers bacteria calculated with qPCR (grey columns) and CFU (dark columns).

3.4. PilE4 interacts with Ig-like C2-type 1 domain of ICAM-1

To reveal amino acid stretches involved in the PilE4:ICAM-1 interface, six truncated forms of ICAM-1 were synthesized. Five truncated ICAM-1 encompassed each of five functional domains. The sixth truncated form, which was used as positive control, contained all five domains (rICAM-1-5). Truncated ICAM-1 were immobilized first on the membrane and then hybridized with PilE4. Among all truncated forms, Ig-like C2-type 1 domain and rICAM-1-5 showed affinity to PilE4 (Fig. 7). These results suggest that PilE4:ICAM-1 dyad formation may be mediated through 1st domain of ICAM-1.

3.5. Inhibition of adhesion by blocking of the ICAM-1 on endothelial cells

To corroborate importance of ICAM-1 in adhesion of *Fth* on endothelial cells, ICAM-1 was blocked with anti-ICAM-1 antibody prior to the incubation with live bacteria. In control wells (no pre-incubation with ICAM-1) we found an average of 5.4×10^5 adherent *Fth* (DNA copy numbers in qPCR; standard deviation 0.93×10^3), whereas in case of endothelial cells pre-incubated with anti-ICAM-1 antibody, we found significant decrease ($P < 0.05$) in the number of adherent bacteria (average 1.02×10^3, standard deviation 1.6×10^2). These results were also corroborated with CFU count (Fig. 8). Pre-incubation of endothelial cells with non-relevant antibodies (anti-CD40 and anti-ZO-1) did not cause reduction in the number of adherent *Fth*. Results indicate that the ICAM-1 molecule is important in the adhesion of *Fth* on endothelial cells, however, it is important to note that adhesion of *Fth* was not completely abrogated in pre-incubated endothelial cells. This suggests that other ligand–receptor interactions may also help *Fth* to adhere to the endothelial cell surface. It is also tempting to speculate that ICAM-1 blocking may not be 100% efficient or during 4 h of incubation with *Fth* new ICAM-1 molecules might have been expressed to the cell surface, whereas previous ICAM-1 blocked with antibody might have been internalized, which account for the residual bacterial adhesion. No adherent bacteria were found in negative controls.

3.6. In silico prediction of PilE4:Ig-like C2-type 1 coupling

The tertiary structures of PilE4 and Ig-like C2-type 1 domain were designed by homology modelling, because the crystal structures of those proteins are unavailable. Although the work of Hartung and colleges determine the structure of PilE of *F. tularensis* [27], the low similarity between the Schu4 and *F. tularensis* subsp. *holarctica* do not allow as use these models as a template for homology modelling. The structure of PilE4 was modelled by MOE software using the 1AL7, 2O8B and 3Qj4 as a templates, which gave the most identity with the sequence. Structurally, PilE4 is composed mainly of a set of a helices and extensive unstructured coils. There is likewise a set of two antiparallel beta-sheet formations near the N-terminal end of the protein. The longest pair of beta-sheets from PilE4 aligns with the extensive interconnected network of antiparallel beta-sheets in the Ig-like C2-type 1 domain. The Ig-like C2-type 1 domain consists of a total of 18 beta-sheets arranged in two main domains, joined by a short loop. Notably only the C-terminal domain of the Ig-like C2-type 1 protein interacts with PilE4, with the exception of a small hairpin loop from the N-terminal domain of Ig-like C2-type 1 protein (Fig. 9).

4. Discussion

To disseminate into the multiple organs, bacteria have to cross various cell barriers including the endothelial barrier present in the blood vessels. Although, *Francisella* prefers intracellular environment, it is also found in the extracellular compartment like the plasma fraction of blood [7,28]. Previously it was reported that 75% of the *Francisella* were present in acellular fraction of the infected mice [7]. Evidence of extracellular multiplication and survival of *Francisella* was also speculated after evidence of the aerosol infection [29]. Till to date, scanty information is available about mechanisms of translocation of extracellular form of *Francisella* across various barriers. Thus an ability of *Fth* to cross the endothelial cell barrier *in vitro* in the absence of leukocytes was assessed in this study. Crossing of the *Fth in vitro* indicates that extracellular form of *Francisella* can translocate endothelial lining either via transcellular or paracellular route. An ability of *Fth* to cross the blood brain barrier and invade extravascular tissues of the brain was also observed in this study. *In vivo* experiment, however, could not shed light on the route of translocation (trans- or paracellular or Trojan

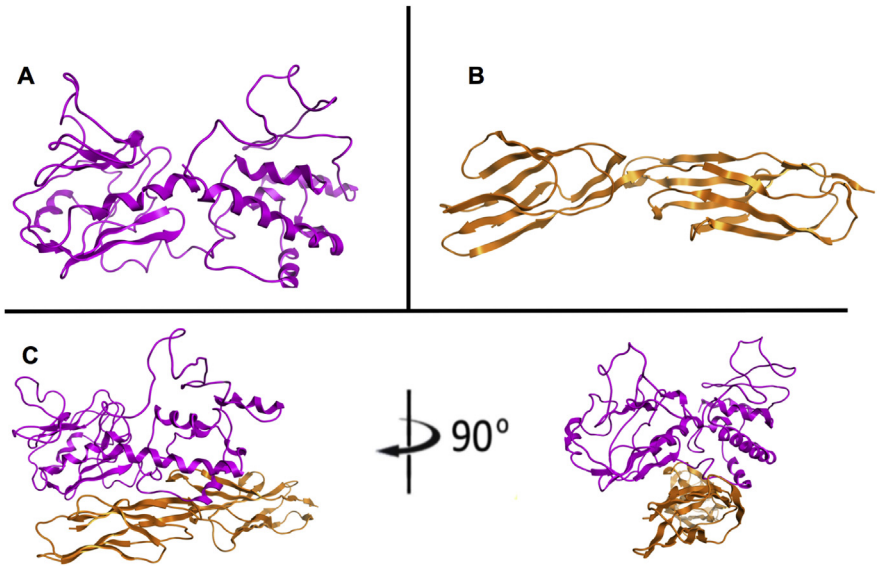

Fig. 9. Homology modelling and molecular docking of the PilE4 and Ig-like C2-type 1 domain. A – the homology model of PilE4, B – the homology model of Ig-like C2-type 1 domain, C – the molecular docking conformation of PilE4 and Ig-like C2-type 1 proteins.

horse) of *Fth* across the barrier. Blood brain barrier is a distinctive and protective wall composed of endothelial cells, astrocytes, basement membrane and pericytes. Though the neuroinvasion of *Francisella* is rare, few reports [1–3] have confirmed the presence of *Francisella* in animal and human brain tissue.

Primary adhesion of extracellular bacteria to the endothelial cells is a crucial step that often evokes rearrangement of the extracellular matrix and may aids bacterial penetration across the barrier [4,5]. Experiments carried out to identify receptor/adhesion molecules on endothelial cells revealed that ICAM-1 is important for *Fth* ligand PilE4. Previously it was reported that type IV pili in other bacteria might promote bacterial adhesion to the endothelial cells and activate signalling pathways. Neisserial PilE subunit is important in pilus-mediated signalling and is required for bacterial aggregation. PilE directly interacts with β2-adrenergic receptor and this interaction leads to penetration of *Neisseria meningitidis* across the endothelial barrier [30]. In case of *Francisella*, importance of type IV pili subunits (*pilF* and *pilT*) for adhesion of bacteria to macrophages, pneumocytes and hepatocytes was described elsewhere [14]. Experiments performed to identify protein/s of *Francisella* interacting with ICAM-1 revealed that PilE4 of *Fth* is the only interacting candidate among type IV pili subunits included in this study (i.e. PilE1, PilE3, PilE4, PilE5 and PilW).

Previously it was shown that the PilE4 coding sequences from LVS and OSU18 (isogenic strain) differ in the encoded subunits [31]. Predicted length of PilE4 in LVS is 301 aa, whereas in OSU18 it is truncated to 211 aa that leads to the heterology at C terminus. Authors also predicted that longer form of PilE4 could be found in low-virulence strains (LVS), and a shorter truncated form in high-virulence (OSU18) strains [31]. It is interesting to note that PilE4 of LVS was also able to interact with ICAM-1 [32]. Furthermore, we also observed that LVS adheres and translocate across BBB *in vitro* (unpublished data). The recombinant PilE4 of LVS used in our previous work [32] and PilE4 of *Fth* in the present study comprised of first 158 aa homologous residues. This suggests that C terminal heterology caused due to the deletions in PilE4 coding sequence (as shown in [31]) may not affect the interaction between PilE4 and ICAM-1.

Identification of the interface between ligand and receptor is important to know the molecular basis of the interaction and it often helps in the development of antimicrobial therapeutics. Thus, attempts were made to identify PilE4 binding domain of ICAM-1. This integrin consists of five immunoglobulin superfamily domains, which comprise of a sandwich of two antiparallel β-sheets stabilized by conserved disulfide bonds [33]. The first domain seems to be an essential ligand-binding site, as it interacts with LFA-1, MAC-1 and fibrinogen and mediates leukocyte adhesion to vascular endothelium [34]. Second domain binds fibrinogen, while the third and fourth domains facilitates site for macrophage-1 antigen (Mac-1, CD11b/CD18) and CD11c/CD18 attachment, respectively. The fifth domain is essential for dimerization of ICAM-1 on the cell surface [35]. We demonstrated that PilE4 of *Fth* interacts with ICAM-1 through Ig-like C2-type 1 domain. Moreover, *in silico* prediction of the PilE4:Ig-like C2-type 1 coupling revealed that C-terminal part of this domain is important in the interaction with PilE4. The first domain has also been described as a receptor for human rhinoviruses and mediates viral uncoating during cell entry [36].

Earlier it was reported that P5 fimbriae of *Haemophilus influenzae* mediates binding to ICAM-1 through Ig-like C2 type 1 or 2 domain and increases expression of ICAM-1 on epithelial cells [37]. Similarly, increased expression of ICAM-1 in the endothelial cells after challenge with neuroinvasive *Borrelia* was reported [15]. Work performed by Forestal and co-workers showed upregulation of ICAM-1 and proinflammatory molecules in the endothelial cells infected with *Francisella* [38]. Role of ICAM-1 in the adhesion of other pathogens like West Nile virus and *H. influenza* was reported previously. Blocking of ICAM-1 molecule caused decrease in adhesion of both pathogens to the cells [37,39]. Similar results were also noted in our study, wherein significant reduction (approximately 500–fold) in the adhesion of *Fth* was observed in endothelial cells pre-incubated with anti-ICAM-1 antibody.

It should be noted that pathogens might express multiple surface proteins to interact with host cells and immune system. They might possess various ligands to adhere to the endothelial and epithelial cell surface. Apart from the PilE4:ICAM-1 interaction, other ligand–receptor interactions might help *Francisella* to adhere to the endothelial surface. In the parallel experiments we showed that OmpA-like protein of *F. tularensis subsp. holarctica* (LVS) also interacts with ICAM-1 [40]. Further study is still ongoing to identify

OmpA-ICAM-1 interface and understand biological significance of this interaction.

Significant reduction in the number of adherent *Fth* in anti-ICAM-1 treated endothelial cells although suggests important role of this integrin in the adhesion of *Francisella*, an average of 1.02×10^3 adherent bacteria on pre-incubated endothelial cells may indicate involvement of other ligand–receptor interaction in the adhesion of *Fth*. More sensitive methods can be used to explore such hidden protein–protein interactions.

In summary, this study presents one of the major ligand:receptor interactions in the adhesion of *Francisella* on the endothelial cell surface. Results also show that extracellular form of *Fth* is able to cross the endothelial barrier without the help of leukocytes. Study also show that *Fth* can cross the endothelial barrier in the brain microvasculature. Further research is needed to explore interactions between extracellular form of *Francisella* and host cells.

Acknowledgements

This work was performed in collaboration with Dr. E. Chakurkar, at ICAR Goa India, mainly for transfection and *in vivo* protein production. Authors thank prof. D. Eckersall, University of Glasgow for correcting the English grammar and reviewing scientific content of the manuscript. This work was supported by academic grants APVV-0036-10 and VEGA–1/0054/12. EB, LP and ZF are funded by ITMS 26220220185.

References

[1] N. Gangat, Cerebral abscesses complicating tularemia meningitis, Scand. J. Infect. Dis. 39 (2007) 258–261.
[2] C.H. Park, A. Nakanishi, H. Hatai, D. Kojima, T. Oyamada, H. Sato, et al., Pathological and microbiological studies of Japanese Hare (*Lepus brachyurus angustidens*) naturally infected with *Francisella tularensis subsp. holarctica*, J. Vet. Med. Sci. Jpn. Soc. Vet. Sci. 71 (2009) 1629–1635.
[3] C. Abril, H. Nimmervoll, P. Pilo, I. Brodard, B. Korczak, S. Markus, et al., Rapid diagnosis and quantification of *Francisella tularensis* in organs of naturally infected common squirrel monkeys (*Saimiri sciureus*), Vet. Microbiol. 127 (2008) 203–208.
[4] L. Pulzova, M.R. Bhide, K. Andrej, Pathogen translocation across the blood-brain barrier, FEMS Immunol. Med. Microbiol. 57 (2009) 203–213.
[5] E. Bencurova, P. Mlynarcik, M. Bhide, An insight into the ligand-receptor interactions involved in the translocation of pathogens across blood-brain barrier, FEMS Immunol. Med. Microbiol. 63 (2011) 297–318.
[6] K.S. Kim, Microbial translocation of the blood-brain barrier, Int. J. Parasitol. 36 (2006) 607–614.
[7] C.A. Forestal, M. Malik, S.V. Catlett, A.G. Savitt, J.L. Benach, T.J. Sellati, et al., *Francisella tularensis* has a significant extracellular phase in infected mice, J. Infect. Dis. 196 (2007) 134–137.
[8] A. Melillo, D.D. Sledjeski, S. Lipski, R.M. Wooten, V. Basrur, E.R. Lafontaine, Identification of a *Francisella tularensis* LVS outer membrane protein that confers adherence to A549 human lung cells, FEMS Microbiol. Lett. 263 (2006) 102–108.
[9] S.R. Lindemann, M.K. McLendon, M.A. Apicella, B.D. Jones, An in vitro model system used to study adherence and invasion of *Francisella tularensis* live vaccine strain in nonphagocytic cells, Infect. Immun. 75 (2007) 3178–3182.
[10] J.G. Moreland, J.S. Hook, G. Bailey, T. Ulland, W.M. Nauseef, *Francisella tularensis* directly interacts with the endothelium and recruits neutrophils with a blunted inflammatory phenotype, Am. J. Physiol. Lung Cell. Mol. Physiol. 296 (2009) L1076–L1084.
[11] A.E. Deghmane, S. Petit, A. Topilko, Y. Pereira, D. Giorgini, M. Larribe, et al., Intimate adhesion of *Neisseria meningitidis* to human epithelial cells is under the control of the crgA gene, a novel LysR-type transcriptional regulator, EMBO J. 19 (2000) 1068–1078.
[12] H. Gil, J.L. Benach, D.G. Thanassi, Presence of pili on the surface of *Francisella tularensis*, Infect. Immun. 72 (2004) 3042–3047.
[13] E.L. Zechner, S. Lang, J.F. Schildbach, Assembly and mechanisms of bacterial type IV secretion machines, Philos. Trans. R. Soc. Lond. B Biol. Sci. 367 (2012) 1073–1087.
[14] S. Chakraborty, M. Monfett, T.M. Maier, J.L. Benach, D.W. Frank, D.G. Thanassi, Type IV pili in *Francisella tularensis*: roles of pilF and pilT in fiber assembly, host cell adherence, and virulence, Infect. Immun. 76 (2008) 2852–2861.
[15] L. Pulzova, A. Kovac, R. Mucha, P. Mlynarcik, E. Bencurova, M. Madar, et al., OspA-CD40 dyad: ligand-receptor interaction in the translocation of neuroinvasive *Borrelia* across the blood-brain barrier, Sci. Rep. 1 (2011) 86.
[16] J.M. Timpe, M.M. Holm, S.L. Vanlerberg, V. Basrur, E.R. Lafontaine, Identification of a *Moraxella catarrhalis* outer membrane protein exhibiting both adhesin and lipolytic activities, Infect. Immun. 71 (2003) 4341–4350.
[17] S. Bergmann, A. Lang, M. Rohde, V. Agarwal, C. Rennemeier, C. Grashoff, et al., Integrin-linked kinase is required for vitronectin-mediated internalization of *Streptococcus pneumoniae* by host cells, J. Cell Sci. 122 (2009) 256–267.
[18] M.R. Bhide, R. Escudero, E. Camafeita, H. Gil, I. Jado, P. Anda, Complement factor H binding by different Lyme disease and relapsing fever *Borrelia* in animals and human, BMC Res. Notes 2 (2009) 134.
[19] E. Bencurova, M. Bhide, Protein Immobilization in Practice: Rapid Protein-protein Interaction Using Reverse Line Bloting, in: Nanomaterials: Fundamentals and Applications, 2012. Slovakia.
[20] M. Bhide, K. Bhide, L. Pulzova, M. Madar, P. Mlynarcik, E. Bencurova, et al., Variable regions in the sushi domains 6-7 and 19-20 of factor H in animals and human lead to change in the affinity to factor H binding protein of *Borrelia*, J. Proteomics 75 (2012) 4520–4528.
[21] B.T. Kurien, R.H. Scofield, Multiple immunoblots after non-electrophoretic bidirectional transfer of a single SDS-PAGE gel with multiple antigens, J. Immunol. Methods 205 (1997) 91–94.
[22] P. Mlynarcik, E. Bencurova, M. Madar, R. Mucha, L. Pulzova, S. Hresko, et al., Development of simple and rapid elution methods for proteins from various affinity beads for their direct MALDI-TOF downstream application, J. Proteomics 75 (2012) 4529–4535.
[23] M. Bhide, S. Natarajan, S. Hresko, C. Aguilar, E. Bencurova, Rapid in vitro protein synthesis pipeline: a promising tool for cost-effective protein array design, Mol. Biosyst. 10 (2014) 1236–1245.
[24] A. Sali, L. Potterton, F. Yuan, H. van Vlijmen, M. Karplus, Evaluation of comparative protein modeling by MODELLER, Proteins 23 (1995) 318–326.
[25] D. Vlachakis, V.L. Koumandou, S. Kossida, A holistic evolutionary and structural study of flaviviridae provides insights into the function and inhibition of HCV helicase, Peer J. 1 (2013) e74.
[26] R. Chen, L. Li, Z.Z.D.O.C.K. Weng, an initial-stage protein-docking algorithm, Proteins 52 (2003) 80–87.
[27] S. Hartung, A.S. Arvai, T. Wood, S. Kolappan, D.S. Shin, L. Craig, et al., Ultrahigh resolution and full-length pilin structures with insights for filament assembly, pathogenic functions, and vaccine potential, J. Biol. Chem. 286 (2011) 44254–44265.
[28] A. Sjostedt, Intracellular survival mechanisms of *Francisella tularensis*, a stealth pathogen, Microbes Infect. 8 (2006) 561–567.
[29] E. Bar-Haim, O. Gat, G. Markel, H. Cohen, A. Shafferman, B. Velan, Interrelationship between Dendritic cell trafficking and *Francisella tularensis* dissemination following airway infection, PLoS Pathog. 4 (2008).
[30] M. Coureuil, H. Lecuyer, M.G.H. Scott, C. Boularan, H. Enslen, M. Soyer, et al., Meningococcus Hijacks a beta 2-Adrenoceptor/beta-Arrestin pathway to cross brain microvasculature endothelium, Cell 143 (2010) 1149–1160.
[31] X. Zogaj, S. Chakraborty, J. Liu, D.G. Thanassi, K.E. Klose, Characterization of the *Francisella tularensis* subsp. *novicida* type IV pilus, Microbiology 154 (2008) 2139–2150.
[32] E. Bencurova, P. Mlynarcik, L. Pulzova, A. Kovac, M. Bhide, PilE4 may contributes in the adhesion of *Francisella* to brain microvascular endothelial cells, Farm Anim. Proteomics (2013) 99–102.
[33] C.D. Jun, C.V. Carman, S.D. Redick, M. Shimaoka, H.P. Erickson, T.A. Springer, Ultrastructure and function of dimeric, soluble intercellular adhesion molecule-1 (ICAM-1), J. Biol. Chem. 276 (2001) 29019–29027.
[34] J. Bella, P.R. Kolatkar, C.W. Marlor, J.M. Greve, M.G. Rossmann, The structure of the two amino-terminal domains of human ICAM-1 suggests how it functions as a rhinovirus receptor and as an LFA-1 integrin ligand, Proc. Natl. Acad. Sci. U. S. A. 95 (1998) 4140–4145.
[35] A. Rahman, F. Fazal, Hug tightly and say goodbye: role of endothelial ICAM-1 in leukocyte transmigration, Antioxid. Redox Signal 11 (2009) 823–839.
[36] J. Bella, P.R. Kolatkar, C.W. Marlor, J.M. Greve, M.G. Rossmann, The structure of the two amino-terminal domains of human intercellular adhesion molecule-1 suggests how it functions as a rhinovirus receptor, Virus Res. 62 (1999) 107–117.
[37] V. Avadhanula, C.A. Rodriguez, G.C. Ulett, L.O. Bakaletz, E.E. Adderson, Nontypeable *Haemophilus influenzae* adheres to intercellular adhesion molecule 1 (ICAM-1) on respiratory epithelial cells and upregulates ICAM-1 expression, Infect. Immun. 74 (2006) 830–838.
[38] C.A. Forestal, J.L. Benach, C. Carbonara, J.K. Italo, T.J. Lisinski, M.B. Furie, *Francisella tularensis* selectively induces proinflammatory changes in endothelial cells, J. Immunol. 171 (2003) 2563–2570.
[39] J.F. Dai, P.H. Wang, F.W. Bai, T. Town, E. Fikrig, ICAM-1 participates in the entry of West Nile virus into the central nervous system, J. Virol. 82 (2008) 4164–4168.
[40] R. Mucha, E. Bencurova, M. Cepkova, P. Mlynarcik, M. Madar, L. Pulzova, et al., Adhesion of *Francisella* to endothelial cells is also mediated by OmpA: ICAM-1 interaction, Farm Anim. Proteomics (2012) 94–97.